

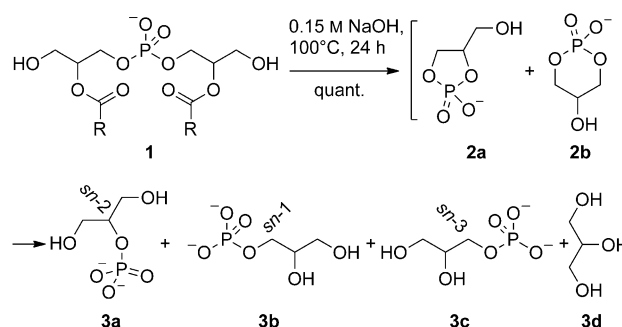
# Spectroscopic Evidence for the Unusual Stereochemical Configuration of an Endosome-Specific Lipid\*\*

Hui-Hui Tan, Asami Makino, Kumar Sudesh, Peter Greimel,\* and Toshihide Kobayashi\*

Glycerophospholipids are essential components of cell membranes from archaea to bacteria and mammals. These lipids feature either an *sn*-3 or *sn*-1 glycerophosphate (GP) backbone. In archaea, glycerophospholipids are exclusively phosphorylated at the *sn*-1 position. In contrast, in bacteria and eukaryotic cells phosphorylation is restricted to the *sn*-3 position. It has been proposed that chiral discrimination caused the phase separation of *sn*-1- and *sn*-3-phosphorylated lipids, leading up to the segregation of archaea and bacteria.<sup>[1]</sup> However, the mammalian lipid bis(monoacylglycero)phosphate (**1**, BMP) has been reported to be the only exception, featuring an *sn*-1 GP backbone.<sup>[2]</sup>

BMP, also known as lysobisphosphatidic acid (LBPA), is a minor constituent of most animal tissues.<sup>[3]</sup> Despite the low overall BMP content of less than one percent of the total phospholipids fraction, BMP is highly enriched in specific membrane domains of late endosomes (LEs).<sup>[4,5]</sup> In LEs endocytosed lipids and proteins, for example, are either recycled or destined for degradation. BMP has been proposed to play an important role in structural and functional aspects of LEs.<sup>[6]</sup>

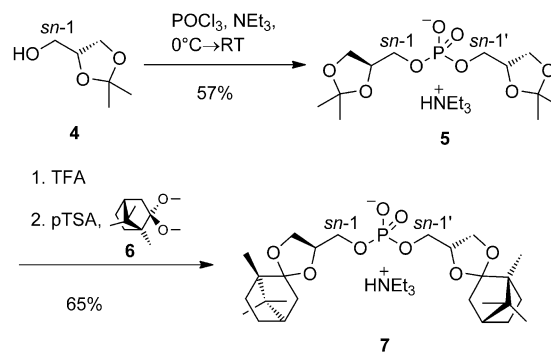
BMP is a structural isomer of phosphatidylglycerol, featuring two glycerol subunits linked by a phosphodiester group. The stereochemical configuration of the diglycerophosphate (DGP) backbone of BMP was biochemically analyzed (Scheme 1).<sup>[2]</sup> During strong alkaline hydrolysis of the phosphate diester group the cyclic intermediates **2a** and **2b** were formed, leading to achiral *sn*-2 GP **3a** as the main product devoid of any stereochemical information. The ratio of **3a** to the mixture of **3b** and **3c** was determined by gas-liquid chromatography. The ratio of **3b** to **3c** was determined by selective digestion of **3c** with glycerol-3-phosphate dehydrogenase. Owing to the harsh cleavage conditions and the indirect detection, Brotherus et al.<sup>[2]</sup> could not exclude the presence of up to 20% *sn*-2 or *sn*-3 phosphorylation in natural BMP.



**Scheme 1.** Strong alkaline degradation of natural BMP during biochemical analysis.<sup>[2]</sup>

To date, no spectroscopic evidence of the stereochemical configuration of the DGP backbone of BMP has been reported. Despite the presence of two stereogenic centers in the DGP backbone, direct NMR spectroscopic identification of the stereochemical configuration has not been conclusive. We envisaged the use of *D*-camphor ketals as NMR shift reagents to directly determine the stereochemical configuration of the BMP backbone. For comparison, we synthesized all three DGP backbone analogues of BMP.

Previous synthetic approaches to BMP employed phosphorus(III)-based chemistry in combination with a protecting group at the phosphate moiety.<sup>[7]</sup> We envisaged the utilization of classic phosphorus(V)-based chemistry to furnish symmetrical DGPs **7** and **10** (Scheme 2 and Scheme 3). In contrast, access to *meso*-DGP **17** (Scheme 5) was pictured utilizing an H-phosphonate monoester as a key intermediate. While P<sup>V</sup>-based chemistry allowed a short synthetic route to **7** and **10**, the P<sup>III</sup>-based chemistry provided the necessary control for the selective introduction of each



**Scheme 2.** Synthesis of *sn*-1,1' DGP **7**. TFA = trifluoroacetic acid, pTSA = *p*-toluenesulfonic acid.

[\*] H.-H. Tan, Dr. A. Makino, Dr. P. Greimel, Dr. T. Kobayashi  
Lipid Biology Laboratory, ASI RIKEN  
351-0198 (Japan)  
E-mail: petergreimel@riken.jp  
kobayashi@riken.jp

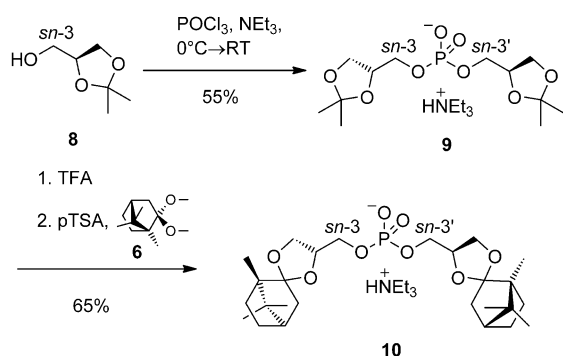
H.-H. Tan, Dr. K. Sudesh, Dr. P. Greimel, Dr. T. Kobayashi  
School of Biological Sciences, Universiti Sains Malaysia  
11800 (Malaysia)

[\*\*] This work was supported by the Lipid Dynamics Program of RIKEN, Naito Foundation (T.K.) and KAKENHI 22390018 (T.K.) & 21790105 (A.M.) from MEXT. H.H.T. thanks the USM Fellowship & RIKEN IPA program for financial support. TOC micrograph by M. Murate.

Supporting information for this article is available on the WWW under <http://dx.doi.org/10.1002/anie.201106470>.

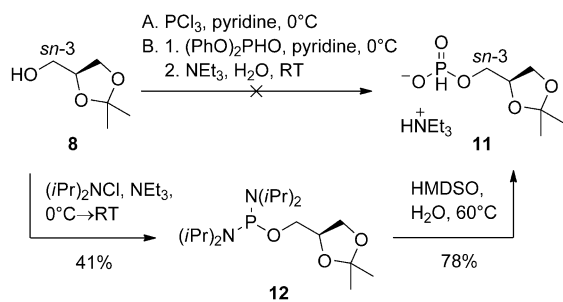
glycerol enantiomer to furnish **17**. Moreover, we omitted the introduction of a protecting group at the phosphate moiety to further reduce the number of synthetic steps.

The symmetrical *sn*-1,1' DGP (**7**) was prepared from 2,3-*O*-isopropylidene-*sn*-glycerol (**4**, Scheme 2). Treatment of alcohol **4** with phosphoryl chloride gave the desired phosphate diester **5**. Transketalization of this intermediate in the presence of *D*-camphor dimethyl ketal (**6**) afforded *D*-camphor bisketal **7**. Even a large excess of **6** and prolonged reaction times of up to seven days resulted in very low yields. The yield was significantly increased by utilizing a two-step, one-pot sequence. First, the isopropylidene protecting group was removed with neat TFA, and the residue was treated with **6** to form desired *sn*-1,1' DGP (**7**). The symmetrical *sn*-3,3' DGP (**10**) was prepared by the same route (Scheme 3), starting from 1,2-*O*-isopropylidene-*sn*-glycerol (**8**).



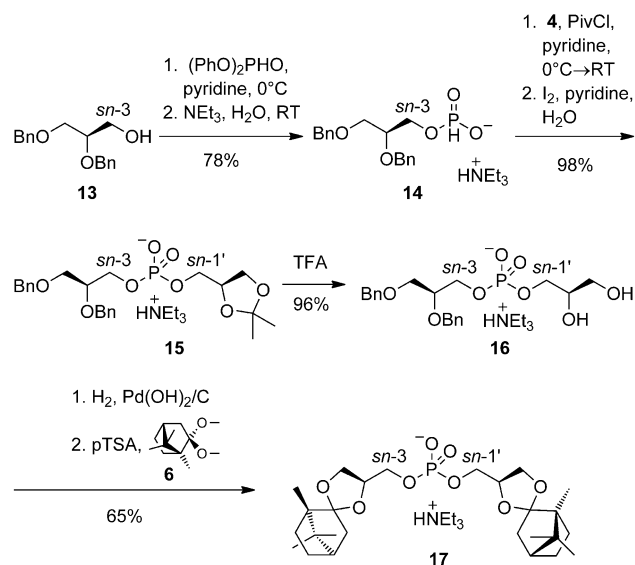
Scheme 3. Synthesis of *sn*-3,3' DGP **10**.

Our initial route (Scheme 4) towards the remaining *meso* analogue **17** required the direct H-phosphonylation of **8**. Treatment of **8** with diphenyl phosphite afforded only undesired phenyl phosphite and phosphorous acid. In the case of phosphorous trichloride, only small amounts of **11** were isolated. In contrast, **8** was readily converted to the phosphordiamidite **12**. Careful hydrolysis of **12** gave crude **11**. Further purification of **11** failed, because of its high susceptibility to hydrolysis. Unfortunately, the presence of small amounts of alcohol **8** in crude **11** rendered this approach unsuitable to access enantiomerically pure *meso*-DGP **17**.



Scheme 4. Synthesis of H-phosphonate **11**. HMDSO = hexamethyldisiloxane.

In light of these results, we adopted an alternative approach (Scheme 5) to **17**. In contrast to isopropylidene-protected **8**, diphenyl phosphite treatment of benzyl-pro-



Scheme 5. Synthesis of *sn*-3,1' DGP **17**. PivCl = pivaloyl chloride.

tected **13** gave H-phosphonate **14** in good yield. Contrary to isopropylidene-protected **11**, benzyl-protected **14** exhibited considerable stability against hydrolysis, easily tolerating chromatographic purification. Subsequently, **15** was prepared by a one-pot condensation-oxidation procedure.<sup>[8]</sup> After the pivaloyl chloride mediated activation of **14**, iodine-mediated oxidation of the mixed phosphonate diester intermediate was performed. The isopropylidene protection was removed by neat TFA giving **16**. After hydrogenolysis, the crude intermediate was treated with **6** to give desired *meso* *D*-camphor bisketal **17**.

The <sup>1</sup>H NMR spectra of bisketals **7** and **10** revealed the presence of a pair of diastereomers, owing to the nonstereospecific formation of the chiral camphor ketals. In contrast, the asymmetric nature of bisketal **17** gave rise to four diastereomers in total. The most prominent shift differences between bisketals **7**, **10**, and **17** are those observed from  $\delta = 4.50$  to 3.70 ppm (Figure 1A–C). In general, the *sn*-2/2' protons exhibit the strongest low-field shift, in the range of  $\delta = 4.50$  to 4.27 ppm. The signals of the glycerol CH<sub>2</sub> protons adjacent to the phosphate moiety are centered around  $\delta = 4.25$  and 4.15 ppm. All signals of terminal protons of the DGP backbones emerge between  $\delta = 3.98$  and 3.70 ppm.

Despite the considerable similarity of the <sup>1</sup>H NMR spectra of bisketals **7**, **10**, and **17**, each spectrum exhibits a distinct pattern. In short, a signal at  $\delta = 3.79$  ppm and the absence of any signal between  $\delta = 4.50$  and 4.33 ppm is typical for *sn*-1,1' DGP (Figure 1A). The characteristic signals for *meso*-DGP **17** are centered at  $\delta = 3.82$  and 4.41 ppm (Figure 1C). In contrast, *sn*-3,3' DGP **10** exhibits signals between  $\delta = 4.50$  and 4.33 ppm, whereas the area around  $\delta = 3.82$  ppm

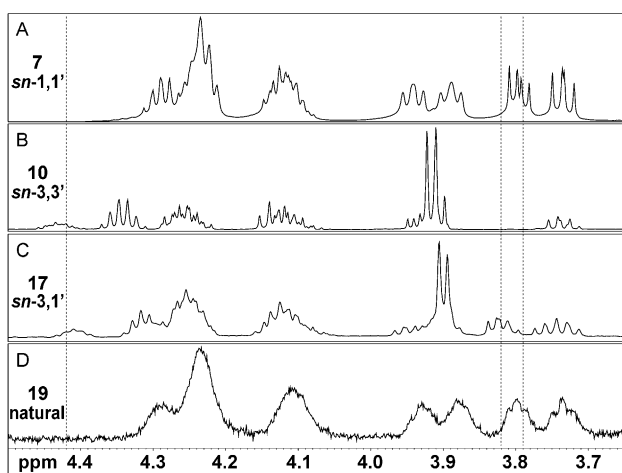
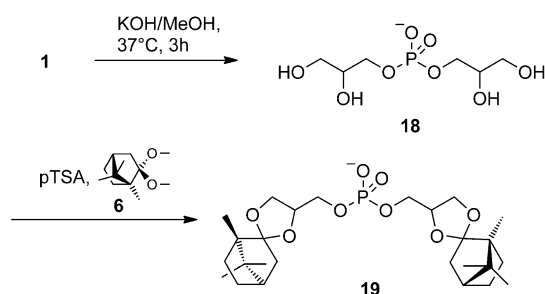


**Figure 1.**  $^1\text{H}$  NMR spectra of the DGP backbone region of d-camphor bisketals in  $[\text{D}_6]\text{benzene}$  A) from *sn*-1,1' DGP **7**, B) from *sn*-3,3' DGP **10**, C) from *sn*-3,1' DGP **17**, and D) from natural BMP **19**. The dashed lines highlight signals at  $\delta = 4.42$ , 3.82, and 3.79 ppm.

as well as around  $\delta = 3.79$  ppm is devoid of any signals (Figure 1 B).

Next, we isolated and purified natural BMP from baby hamster kidney (BHK) cells as described.<sup>[5]</sup> Mass spectrometric analysis revealed that natural BMP from BHK cells predominantly features oleic acid residues (data not shown). To determine the stereochemical configuration of the DGP backbone of isolated BMP (1 mg), we first cleaved the fatty acid residues by mild alkaline methanolysis (Scheme 6). After neutralization by ion-exchange column, the fatty acid methyl esters were removed by hexane extraction. Subsequently, the lyophilized intermediate **18** was converted into its d-camphor bisketal derivative **19** by treatment with an excess of **6** under mild acidic conditions.

Finally, **19** (0.4 mg) was subjected to NMR spectroscopic analysis (Figure 1 D). One of the most prominent aspects of the  $^1\text{H}$  NMR spectrum of **19** is the apparent lack of signals between  $\delta = 4.50$  and 4.33 ppm. Furthermore, only a weak shoulder is present at 3.82, originating from a signal around 3.79 ppm. This signal pattern is in good agreement with the typical features of *sn*-1,1' DGP **7** (Figure 1 A). Interestingly, the presence of other stereoisomers is well below the minimum detection limit of  $^1\text{H}$  NMR spectroscopy.



**Scheme 6.** Conversion of natural BMP (**1**) to its d-camphor bisketal derivative **19**.

In conclusion, we prepared the d-camphor bisketal derivative of natural BMP to identify the stereochemical configuration of its DGP backbone by  $^1\text{H}$  NMR spectroscopy. As reference materials we synthesized the *sn*-1,1', *sn*-3,3', and *sn*-3,1' DGP analogues. Comparison of the  $^1\text{H}$  NMR spectra revealed that natural BMP features the unusual *sn*-1,1' DGP backbone. In contrast to previous biochemical analysis,<sup>[2]</sup> the presence of other DGP backbone configurations in natural BMP was below the minimum detection limit. BMP is enriched in the luminal side of LEs,<sup>[9]</sup> where lipids are exposed to hydrolysis catalyzed by degrading enzymes. The *sn*-1,1' DGP backbone of BMP is advantageous, because phospholipases preferentially hydrolyze *sn*-3 phospholipids. Besides in mammalian cells, the occurrence of BMP has only been reported in alkaliphilic bacteria<sup>[10]</sup> and in the amoeba *Dictyostelium discoideum*.<sup>[11]</sup> Bacterial BMP has been reported to exhibit an *sn*-3,1' DGP backbone,<sup>[10]</sup> whereas the stereochemical configuration of amoeban BMP has not been reported. This observation suggests that *sn*-1 phospholipids, besides in archaea, are restricted to the endocytic organelles of eukaryotic cells. An exciting possibility is that BMP in eukaryotic cells originates from endocytosed archaea.

Received: September 13, 2011

Published online: December 1, 2011

**Keywords:** configuration determination · NMR spectroscopy · phospholipids · structure elucidation

- [1] a) G. Wächtershäuser, *Mol. Microbiol.* **2003**, *47*, 13–22; b) J. Peretó, P. López-García, D. Moreira, *Trends Biochem. Sci.* **2004**, *29*, 469–477; c) Y. Koga, *J. Mol. Evol.* **2011**, *72*, 274–282.
- [2] J. Brotherus, O. Renkonen, J. Herrmann, W. Fischer, *Chem. Phys. Lipids* **1974**, *13*, 178–182.
- [3] a) F. Hullin-Matsuda, C. Luquain-Costaza, J. Bouvier, I. Delton-Vandenbroucke, *Prostaglandins Leukotrienes Essent. Fatty Acids* **2009**, *81*, 313–324; b) E. Orsó, M. Grandl, G. Schmitz, *Chem. Phys. Lipids* **2011**, *164*, 479–487.
- [4] T. Kobayashi, E. Stang, K. S. Fang, P. de Moerloose, R. G. Parton, J. Gruenberg, *Nature* **1998**, *392*, 193–197.
- [5] T. Kobayashi et al., *J. Biol. Chem.* **2002**, *277*, 32157–32164, see the Supporting Information.
- [6] a) H. Matsuo et al., *Science* **2004**, *303*, 531–534, see the Supporting Information; b) T. Hayakawa et al., *Biophys. J.* **2007**, *92*, L13–16, see the Supporting Information; c) I. Delton-Vandenbroucke, J. Bouvier, A. Makino, N. Besson, J.-F. Pageaux, M. Lagarde, T. Kobayashi, *J. Lipid Res.* **2007**, *48*, 543–552; d) I. Le Blanc et al., *Nat. Cell Biol.* **2005**, *7*, 653–664, see the Supporting Information.
- [7] a) J. Chevallier, N. Sakai, F. Robert, T. Kobayashi, J. Gruenberg, S. Matile, *Org. Lett.* **2000**, *2*, 1859–1861; b) G. Jiang, Y. Xu, T. Falguieres, J. Gruenberg, G. D. Prestwich, *Org. Lett.* **2005**, *7*, 3837–3840; c) G. Jiang, Y. Xu, G. D. Prestwich, *J. Org. Chem.* **2006**, *71*, 934–939.
- [8] P. Greimel, M. Lapeyre, Y. Nagatsuka, Y. Hirabayashi, Y. Ito, *Bioorg. Med. Chem.* **2008**, *16*, 7210–7217.
- [9] T. Kobayashi, K. Startchev, A. J. Whitney, J. Gruenberg, *Biol. Chem.* **2001**, *382*, 483–485.
- [10] M. Nishihara, H. Morii, Y. Koga, *J. Biochem.* **1982**, *92*, 1469–1479.
- [11] J. M. Rodriguez-Paris, K. V. Nolte, T. L. Steck, *J. Biol. Chem.* **1993**, *268*, 9110–9116.